Article:

Pritchard, VE, Martir, DR, Oldknow, S et al. (5 more authors) (2017) Homochiral self-sorted and emissive Ir(III) metallo-cryptophanes. Chemistry - A European Journal, 23 (26). pp. 6290-6294. ISSN 0947-6539

https://doi.org/10.1002/chem.201701348

Homochiral self-sorted and emissive Ir(III) metallo-cryptophanes

Victoria E. Pritchard,[a] Diego Rota Martir,[b] Samuel Oldknow,[a] Shumpei Kai,[c] Shuichi Hiraoka,[c] Nikki J. Cookson,[a] Eli Zysman-Colman*,[b] and Michaele J. Hardie*[a]

Dedicated to the memory of Dr Julie Fisher.

Abstract: The racemic ligands (±)-tris(isonicotinoyl)-cyclotriguaiacylene (L1), or (±)-tris(4-pyridyl-methyl)-cyclotriguaiacylene (L2) assemble with racemic (Λ,Δ)-$[Ir(ppy)_2(MeCN)_2]^+$ where ppy = 2-phenylpyridinato to form $[\{Ir(ppy)_2\}_3(L)_2]^{3+}$ metallo-cryptophane cages. The crystal structure of $[\{Ir(ppy)_2\}_3(L1)_2]\cdot 3BF_4$ has MM-ΛΛΛ and PP-ΔΔΔ isomers, and homochiral self-sorting occurs in solution, a process accelerated by a chiral guest. Self-recognition between L1 and L2 within cages does not occur, and cages show very slow ligand-exchange. Both cages are phosphorescent, with $[\{Ir(ppy)_2\}_3(L2)_2]^{3+}$ having enhanced and blue-shifted emission when compared with $[\{Ir(ppy)_2\}_3(L1)_2]^{3+}$.

Metallo-cages are discrete 3-D coordination assemblies with a hollow interior with applications as hosts and nanoscale vessels.[1] They form through the self-assembly of multidentate ligands with metals, or with metal complexes with controlled available coordination sites (“metallo-tectons”). Luminescent metallo-cages are known,[2-6] with most examples exhibiting fluorescence-active ligands,[2] alongside rarer examples of cages with pendant metal-complex emissive groups.[3] There are very few examples of metallo-cages constructed from inherently phosphorescent structural components.[4-6] Cyclometalated Ir(III) complexes bearing either two N-donor ligands or one N^N chelating ligand represent an important subclass of phosphorescent materials.[7] Lusby et al reported the enantiopure Ir(III) metallo-cage $[\{Ir(ppy)_2\}_6(tcb)_4]\cdot(OTf)_6$ (tcb = 1,3,5-tricyanobenzene) [4] which self-assembles, despite the inertness of the d^6 Ir(III) center, as the C,C-cis-N,N-trans arrangement of the ppy ligands has a trans labilising effect. The cage show red-shifted emission compared with a monomeric analogue, and enhanced photoluminescence quantum yields (Φ_{PL}). To date, this is the only report of a 3-D metallo-cage that utilizes $[Ir(ppy)_2]$ as the sole metal centre, although mixed metal examples are known.[5]

[a] Dr V. E. Pritchard, S. Oldknow, Dr N. J. Cookson, Prof. M. J. Hardie
School of Chemistry
University of Leeds
Woodhouse Lane, Leeds LS2 9JT, UK
E-mail: m.j.hardie@leeds.ac.uk
[b] D. Rota Martir, Dr E. Zysman-Colman
Organic Semiconductor Centre, EaSTCHEM School of Chemistry
University of St Andrews
St Andrews, Fife KY16 9ST, UK
E-mail: eli.zysman-colman@st-andrews.ac.uk
[c] S. Kai, Prof S. Hiraoka
Department of Basic Science
Graduate School of Arts and Sciences
The University of Tokyo
3-8-1 Komaba, Meguro-ku, Tokyo 153-8902, Japan

Supporting information for this article is given via a link at the end of the document.

We report herein two metallo-cages of the type $[\{Ir(ppy)_2\}_3(L)_2]^{3+}$ where L is a chiral tripodal ligand related to the molecular host cyclotriveratrylene (CTV). $\{M(chelate)\}_3L_2$ cages with CTV-type ligands are known as metallo-cryptophanes, and most examples feature square planar metals.[8] The $[\{Ir(ppy)_2\}_3(L)_2]^{3+}$ cages reported here show homochiral sorting on crystallization and in solution, and slow ligand exchange behavior is observed.

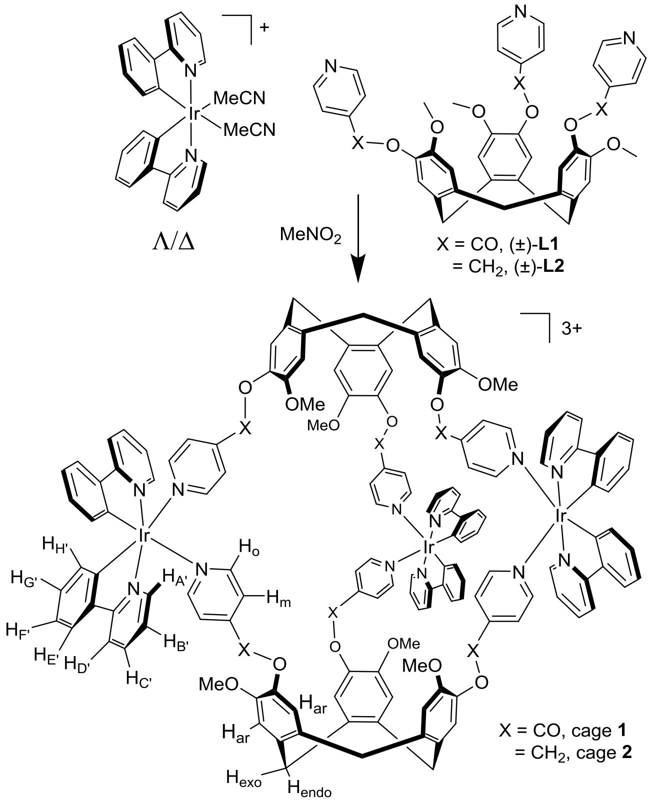

Scheme 1. Synthesis of metallo-cryptophane cage species.

Cages $[\{Ir(ppy)_2\}_3(L1)_2]^{3+}$ **1** and $[\{Ir(ppy)_2\}_3(L2)_2]^{3+}$ **2** are formed from nitromethane mixtures of (Λ,Δ)-$[Ir(ppy)_2(MeCN)_2]\cdot X$ ($X = PF_6^-$, BF_4^-) and (±)-L1 or (±)-L2 in 3:2 stoichiometry, Scheme 1. Electrospray ionization mass spectrometry (ESI-MS) gives a triply charged m/z peak at 983.1120 (cage **1**) or at 955.2853 (cage **2**), along with $[\{Ir(ppy)_2\}(L)]^{3+}$ and $[\{Ir(ppy)_2\}_2(L)_2]^{3+}$ fragment species (SI Figs. S3, S4). Initial ^{1}H NMR of $[Ir(ppy)_2(NCMe)_2]\cdot X$ and L in d_3-$MeNO_2$ show considerable broadening of the resonances and chemical shift changes, most saliently the ppy protons ortho to the coordinating N ($H_{A'}$) and C ($H_{H'}$) move upfield and downfield, respectively, and for cage **2** the previously sharp CH_2 bridge singlet of L2 at 5.19 ppm becomes a complex multiplet as free rotation is hindered (Fig. S15). ROESY spectra of **1** and **2** give expected couplings, including between $H_{H'}$ on the ppys and the ortho pyridyl protons of L (Figs. S8, S16). Diffusion ordered NMR in d_3-$MeNO_2$ for **1**·$3PF_6$ (Fig. S9) gave a hydrodynamic radius of 18.99 Å.

The structure of **1**·$3BF_4$·n($MeNO_2$) was confirmed by crystallography, Fig. 1.[9] There are two independent cage **1** cations that show minor structural differences. Anions and additional solvent were not located due to significant disorder. Each cage has three pseudo-octahedrally coordinated Ir(III) centers, each with two ppy ligands and the pyridyl groups from two L1 ligands in a cis arrangement. The two L1 ligands bridge between three Ir(III) centers. Average torsion angle between cis pyridyl groups is 38.04°, typical for $[Ir(ppy)_2(pyridyl)_2]$-type complexes [10] with the bowl shape of CTV-type ligands able to accommodate these torsion angles within the cage structure.

Both L1 ligands within each cage **1** are the same enantiomer, giving the chiral anti-cryptophane isomer. Each $[Ir(ppy)_2]$ unit within a cage has the same chirality, such that only the enantiomeric MM-ΛΛΛ and PP-ΔΔΔ cage isomers are observed in the structure. Given the Λ and Δ enantiomers of the $[Ir(ppy)_2]^+$ moieties and the M and P enantiomers of the L-types ligands are present in the reaction mixture, there are twelve possible stereoisomers of the cage.

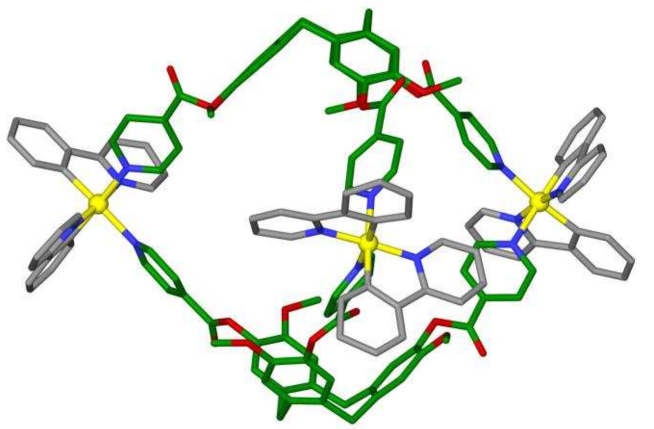

Figure 1. A $[\{Ir(ppy)_2\}_3(L1)_2]^{3+}$ cage from the crystal structure of **1**·$3BF_4$·n(CH_3NO_2), L1 and ppy ligands shown in green and grey respectively.

The ^1H NMR spectra of both cages **1** and **2** undergo significant sharpening upon standing (Figs. S7 and S15), and fully equilibrate after several months. The ^1H NMR spectrum of cage **1**·$3PF_6$ collected after 3 months of standing is virtually identical to that of the single crystals of **1**·$3BF_4$·n(CH_3NO_2) re-dissolved in d_3-$MeNO_2$, Fig. 2a/b. (±)-L1 was resolved into its constituent enantiomers by chiral HPLC,[11] and each L1 enantiomer reacted with each of Λ-$[Ir(ppy)_2(MeCN)_2]$·BF_4 and Δ-$[Ir(ppy)_2(MeCN)_2]$·BF_4. As expected, two combinations were mis-matched pairs of enantiomers that gave poorly resolved ^1H NMR spectra (Figs. S10-11) while two combinations were matched pairs (presumably M-Δ and P-Λ) gave sharp spectra in short timeframes that were similar to the fully sorted cage mixture (Figs. 2d, S12-13). ESI-MS of matched and mis-matched pairs are similar with all combinations showing cage formation (Fig. S14). The observed ^1H NMR spectral sharpening is therefore indicative of equilibration involving chiral self-sorting of an initial mixture of cage stereoisomers, as was also seen in our previous studies of a $[Pd_6(L1)_8]^{12+}$ cage but where only the ligand was a chiral component.[12] We could not resolve the sorted cages by analytical chiral HPLC.

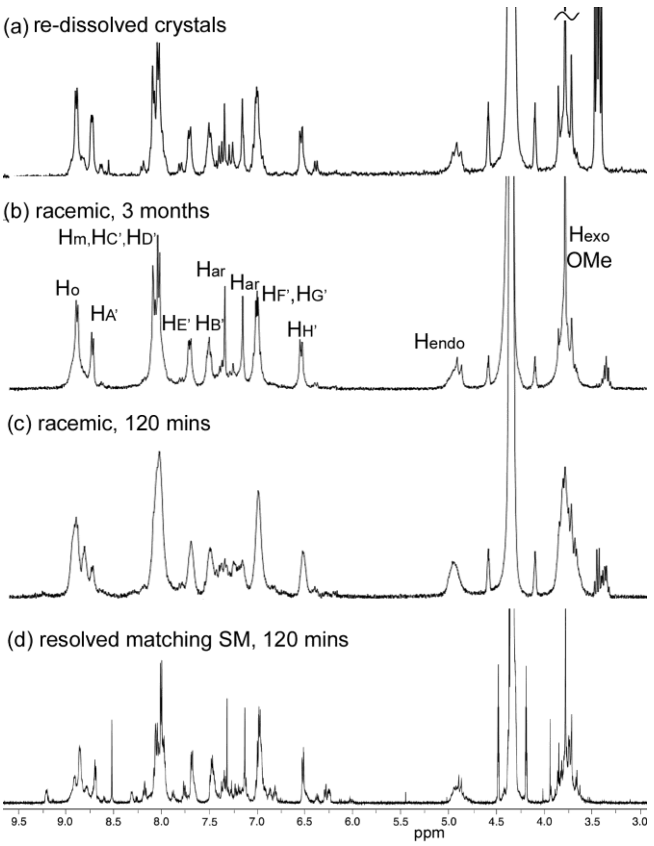

Figure 2. ^1H NMR spectra of cage **1** in CD_3NO_2 of (a) re-dissolved racemic single crystals of MM-ΛΛΛ and PP-ΔΔΔ cages of **1**·$3BF_4$; (b) (Λ,Δ)-$[Ir(ppy)_2(MeCN)_2]$·PF_6 and (±)-L1 3 months after mixing; (c) (Λ,Δ)-$[Ir(ppy)_2(MeCN)_2]$·PF_6 and (±)-L1 two hours after mixing; (d) matched pair of Δ-$[Ir(ppy)_2(MeCN)_2]^+$ and one L1 enantiomer after 2 hrs.

Homochiral metallo-cages with tris-chelate metal coordination are known both from achiral [13a-b] and resolved chiral ligands.[13c-e] Metallo-cages that show homochiral self-sorting from a racemic mixture of ligand enantiomers observed in solution are rare,[14] though include Pd(II) metallo-cryptophanes.[8a] The simultaneous chiral self-sorting of both ligand and pre-formed inert metallo-tecton as reported here has not been previously reported.

In a preliminary investigation of the influence of chiral guests on the self-assembly of cage **1** globular additives were included in 3:2 mixtures of (Λ,Δ)-$[Ir(ppy)_2(MeCN)_2]$·PF_6 and (±)-L1. Addition of chiral R-camphor or S-camphor led to noticeably faster sharpening of the ^1H NMR spectra than in their absence, but this was not observed for addition of achiral adamantane (Fig. S15-S20). Interestingly, addition of the related anionic species R-(or S-)-10-camphorsulfonic acid to the reaction mixture prevents cage formation presumably as carboxylate is a competing ligand for the iridium (Fig. S21-22).

The cages do not show self-recognition of L-ligand species. ESI-MS of a $MeNO_2$ solution of L1, L2 and $[Ir(ppy)_2(MeCN)_2]$·BF_4 shows a statistical mixture of **1**:$[\{Ir(ppy)_2\}_3(L1)(L2)]^{3+}$:**2** cage species, Fig. 3. Mixing **1**·$3BF_4$ and **2**·$3BF_4$ in $MeNO_2$ results in very slow exchange between L1 and L2 with appreciable ligand

Table 1. Photophysical properties of complexes **1**·3(BF_4) and **2**·3(BF_4).

	λ_{em} (nm)			Φ_{PL}(%)[d]			τ_e (ns)[g]		
	DCM [a,b,f]	film [c,f]	powder	DCM [a]	Film [c,e]	powder [e]	DCM [a]	film [c]	powder
1	604	481 (0.7), 514 (1), 556 (0.8)	648	1	5.5	1.3	59 (0.7), 129 (0.3)	634 (0.4), 2319 (0.6)	55 (0.6), 203 (0.4)
2	485 (0.8), 516 (1), 547 (0.6)	486 (0.8), 515 (1), 545 (0.6)	519	15	10	1.6	523 (0.4), 887 (0.6)	688 (0.7), 3042 (0.3)	141 (0.4), 1175 (0.6)

[a] Measurements in degassed DCM at 298 K. [b] Quinine sulfate employed as the external reference (Φ_{PL} = 54.6% in 0.5 M H_2SO_4 at 298 K). [c] PMMA doped films (5 wt % of cage) formed by spin-coating deposition on quartz substrate. [d] Φ_{PL} measurements were carried out under nitrogen (λ_{exc} = 360 nm). [e] values obtained using an integrating sphere. [f] Principal emission peaks listed with values in brackets indicating relative intensity. [g] λ_{exc} = 378 nm; Values in parentheses are pre-exponential weighting factor, in relative % intensity, of the emission decay kinetics.

exchange only observed after 4 weeks, and near-statistical mixing reached after 10 weeks (Figure S6). Thus these cages have a high degree of kinetic stability but are not completely inert. It is interesting to note that this speciation behavior is in contrast with recently reported $[Pd_3L_2]^{6+}$ metallo-cryptophanes, which exclusively formed homocages from two different L-type ligands, with no ligand exchange.[8a]

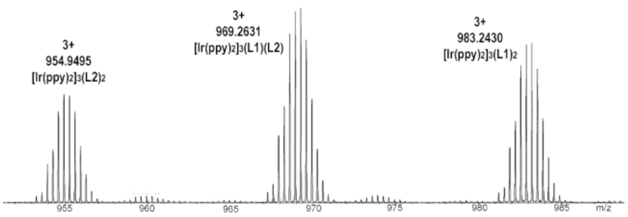

Figure 3. ESI-MS of a 1:1:3 mixture of L1:L2: $[Ir(ppy)_2(MeCN)_2]\cdot BF_4$ in $MeNO_2$ showing formation of statistical mixture of homoleptic and heteroleptic cages.

The absorption spectra of **1** and **2** in dichloromethane (DCM) are similar to other $[Ir(ppy)_2(N^\wedge N)]^+$ systems,[7] and characterised by two intense ligand centered (^{1}LC) transitions between 260 and 320 nm localised on the ppy and three lower intensity broad bands at below 380 nm that consist of spin-allowed and spin-forbidden mixed metal-to-ligand and ligand-to-ligand charge transfer (^{1}MLCT/^{1}LLCT and ^{3}MLCT/^{3}LLCT) transitions (Fig. S26). The weak CT transition observed for **1** at 470 nm was not reported for the monomeric $[Ir(ppy)_2(4\text{-}pyCO_2Et)_2]^+$ (4-$pyCO_2Et$ = 4-ethyl isonicotinate),[10c] pointing to increased conjugation in **1** due to the CTV scaffold. For both **1** and **2**, the excitation spectra in DCM match the absorption spectra and indicate a single photophysically-active species.

Cages **1** and **2** are emissive in DCM solution and in the solid state. Upon photoexcitation of **1**, a broad and unstructured emission is observed both in DCM and in the powder, Fig. 4a**,** due to emission from a mixed ^{3}MLCT/^{3}LLCT state.[7] The photoluminescence spectrum in the powder is red-shifted (λ_{max} = 648 nm) compared to that in DCM (λ_{max} = 604 nm); however, **1** possesses similarly low Φ_{PL} of around 1% and bi-exponential decay kinetics in both media, Table 1. Due to the increased conjugation into the CTV scaffold, cage **1** shows red-shifted emission and similar Φ_{PL} compared to $[Ir(ppy)_2(4\text{-}pyCO_2Et)_2]^+$ (λ_{max} = 560 nm; Φ_{PL} = 2%).[10c] Lusby's $[\{Ir(ppy)_2\}_6(tcb)_4]^{6+}$ cage also showed red-shifted emission (λ_{max} = 575 nm) when compared with the corresponding $[Ir(ppy)_2(NCPh)_2]OTf$ complex (λ_{max} = 525 nm); however, unlike for cage **1** and other $Ir(ppy)_2$ discrete supramolecular systems,[15] the Φ_{PL} for the Lusby cage was enhanced compared with that of the mononuclear complex (Φ_{PL} = 4% cf. Φ_{PL} = < 1%).[4]

In order to mitigate non-radiative vibrational motion in the cage we spin-coated 5 wt % of **1** in polymethyl methacrylate (PMMA), which serves as an inert matrix. The emission in the thin film was blue-shifted and more structured (λ_{max} = 514 nm) compared to both the powder and solution spectra. The Φ_{PL} of 5.5% was enhanced as a result of the rigidification conferred by the PMMA host and the emission lifetimes were significantly longer (τ_e = 634 and 2319 ns).

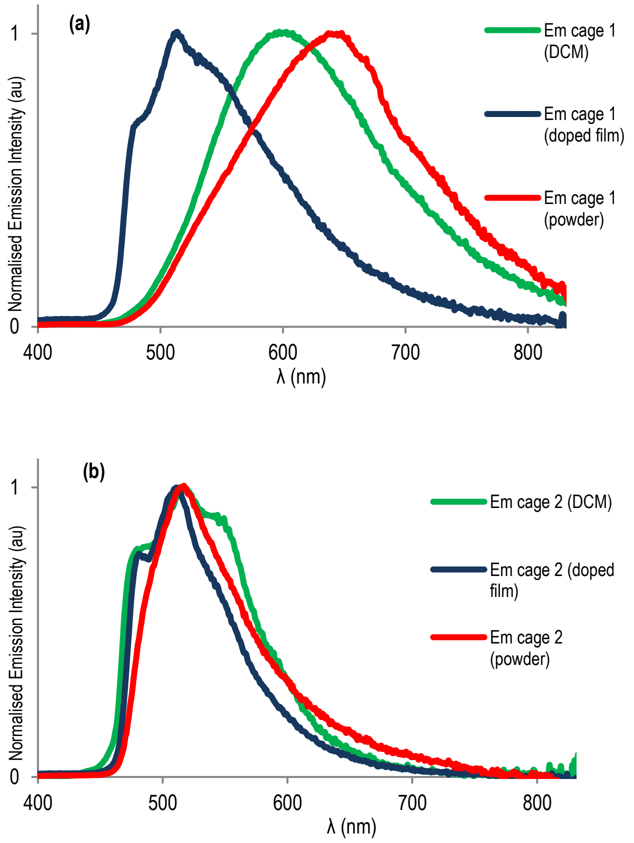

Figure 4. Normalised photoluminescence spectra of a) **1**·$3BF_4$ and b) **2**·$3BF_4$. Dotted lines de-areated DCM solution; dashed lines PMMA doped films with 5 wt % of cages spin-coated on a quartz substrate; red lines bulk powders.

The photoluminescence spectrum of cage **2** in DCM is more structured and blue-shifted (λ_{max} = 516 nm) compared to **1**, indicating emission that is more predominantly ligand-centered (^{3}LC) (Fig. 4(b)). The blue-shifted emission of **2** compared to **1** was expected considering the presence of the electron-withdrawing ester moieties located on L1 in **1**, which stabilise the LUMO.[10c] Cage **2** shows a significantly enhanced Φ_{PL} and longer τ_e compared to **1** in DCM (Φ_{PL} = 15%, τ_e = 523, 887 ns).

Unlike for **1**, as a powder the emission of **2** is not significantly red-shifted (λ_{max} = 519 nm) though the emission profile is less structured, showing less well-resolved vibrational bands as shoulders of the main emission peak. The emission profile for **2** in PMMA doped thin film is likewise very similar to that in DCM. Though Φ_{PL} values are low in the powder (Φ_{PL} = 1.6%), in doped film they are higher (Φ_{PL} = 10 %). Emission lifetimes are expectedly longer in doped films than in powder, Table 1. Attempts to synthesize an analogous mononuclear complex of 4-phenoxymethylpyridine for comparison were not successful due to ligand oligomerization.

In summary, phosphorescent $[\{Ir(ppy)_2\}_3(L)_2]^{3+}$ metallo-cryptophanes can be synthesized in high yields, with the CTV-type ligands able to accommodate torsion angles typical of $[Ir(ppy)_2(L)_2]$ complexes to form rare examples of 3-D Ir(III) cyclometallated coordination cages. These cages undergo ligand exchange processes over months, and show a remarkably high degree of homochiral self-sorting of both ligand and metallo-tecton, but not self-recognition between similar L-type ligands. Chiral sorting is enhanced by the presence of neutral chiral additives. For cage **1** chiral self-sorting occurs relatively rapidly upon crystallization through an induced seeding effect, but on a timescale of months in solution. Luminescence properties of the two cages are quite distinct, pointing to an ability to tune the photophysical properties of these systems. Cage **2** showed an enhanced and blue-shifted emission compared to **1**, reaching a Φ_{PL} of 15% in DCM solution and 10% in doped film. These are promising systems for a variety of applications: as semiochemical hosts, photoredox catalysts and in energy conversion materials.

Acknowledgements

We thank the EPSRC (DTG award 1238852, EP/K039202/1, EP/M02105X/1, EP/J001325/1), Leverhulme Trust (RPG-2014-148), University of St Andrews, and the MEXT/JSPS Grants in Aid for Scientific Research (JP25102005 and JP25102001) for funding; Simon Barrett for assistance with NMR; Martin Huscroft for assistance with HPLC, and Stephen Boyer for elemental analysis measurements.

Data accessibility. Data supporting this work can be accessed at DOI:###########.

Keywords: supramolecular chemistry; cage compounds • homochiral self-sorting • phosphorescence

[1] Reviews: a) S. Zarra, D. M. Wood, D. A. Roberts, J. R. Nitschke, Chem. Soc. Rev. **2015**, 44, 419-432; b) T. R. Cook, Y.-R. Zheng, P. J. Stang, Chem. Rev. **2013**, 113, 734-777; c) K. Harris, M. Fujita, Chem. Commun. **2013**, 49, 6703-6712; d) M. D. Ward, Chem. Commun. **2009**, 4487-4499; e) D. Fiedler, D. H. Leung, R. G. Bergman, K. N. Raymond, Acc. Chem. Res., **2005**, 38, 349-358.

[2] for examples and reviews a) J. R. Piper, L. Cletheroe, C. G. P. Taylor, A. J. Metherell, J. A. Weinstein, I. V. Sazanovich, M. D. Ward, Chem. Commun. **2017**, 53, 408-411; b) A. Schmidt, M. Hollering, M. Drees, A. Casini, F. E. Kühn, Dalton Trans. **2016**, 45, 8556-8565; c) L. Xu, Y.-X. Wang, H.-B. Yang, Dalton Trans. **2015**, 44, 867-890; d) X. Yan, T. R. Cook, P. Wang, F. Huang, P. J. Stang, Nature Chem. **2015**, 7, 342-348; e) J. E. M. Lewis, A. B. S. Elliot, C. J. McAdam, K. C. Gordon, J. D. Crowley, Chem. Sci. **2014**, 5, 1833-1843; f) Z. Li, N. Kishi, K. Yoza, M. Akita, M. M. Yoshizawa, Chem. Eur. J. **2012**, 18, 8358-8365; g) K. Harano, S. Hiraoka, M. Shionoya, J. Am. Chem. Soc. **2007**, 129, 5300-5301; h) N. K. Al-Rasbi, C. Sabatini, F. Barigelletti, M. D. Ward, Dalton Trans. **2006**, 4769-4772.

[3] A. Schmidt, M. Hollering, J. Han, A. Casini, F. E. Kühn, Dalton Trans. **2016**, 45, 12297-12300; b) A. B. S. Elliot, J. E. M. Lewis, H. van der Salm, C. J. McAdams, J. D. Crowley, K. C. Gordon, Inorg. Chem. **2016**, 55, 3440-3447; c) W. J. Ramsay, J. A. Foster, K. L. Moore, T. K. Ronson, R. J. Mirgalet, D. A. Jefferson, J. R. Nitschke, Chem. Sci. **2015**, 6, 7326-7331.

[4] O. Chepelin, J. Ujma, X. Wu, A. M. Z. Slawin, M. B. Pitak, S. J. Coles, J. Michel, A. C. Jones, P. E. Barran, P. J. Lusby, J. Am. Chem. Soc. **2012**, 134, 19334-19337.

[5] a) X. Li, J. Wu, L. Chen, X. Zhong, C. Heng, R. Zhang, C. Duan, Chem. Commun. **2016**, 52, 9628-9631; b) X. Li, J. Wu, C. Heng, R. Zhang, C. Duan, Chem. Commun. **2016**, 52, 5104-5107.

[6] a) C. Shen, A. D. W. Kennedy, W. A. Donald, A. M. Torres, W. S. Price, J. E. Beves, Inorg. Chim. Acta. **2017**, 458, 122-128; b) J. Yang, M. Bhadbhade, W. A. Donald, H. Iranmanesh, E. G. Moore, H. Yan, J. E. Beves, Chem. Commun. **2015**, 51, 4465-4468; c) A. B. Wragg, A. J. Metherell, W. Cullen and M. D. Ward, Dalton Trans. **2015**, 44, 17939-17949; d) K. Li, L.-Y. Zhang, C. Yan, S.-C. Wei, M. Pan, L. Zhang, C.-Y. Su, J. Am. Chem. Soc. **2014**, 136, 4456-4459.

[7] a) D. R. Martir, A. K. Bansal, V. Di Mascio, D. B. Cordes, A. F. Henwood, A. M. Z. Slawin, P. C. J. Kamer, L. Martínez-Sarti, A. Pertegás, H. J. Bolink, I. D. W. Samuel, E. Zysman-Colman, Inorg. Chem. Front. **2016**, 3, 218-235; b) A. M. Bünzli, E. C. Constable, C. E. Housecroft, A. Prescimone, J. A. Zampese, G. Longo, L. Gil-Escrig, A. Pertegás, E. Ortí, H. J. Bolink, Chem. Sci. **2015**, 6, 2843-2852; c) S. Ladouceur, E. Zysman-Colman, Eur. J. Inorg. Chem. **2013**, 2985-3007; d) Y. You, S. Y. Park, Dalton Trans. **2009**, 1267-1282; e) S. Lamansky, P. Djurovich, D. Murphy, F. Abdel-Razzaq, H.E. Lee, C. Adachi, P. E. Burrows, S. R. Forrest, M. E. Thompson J. Am. Chem. Soc. **2001**, 123, 4304-4312.

[8] a) A. Schaly, Y. Rousselin, J.-C. Chambron, E. Aubert, E. Espinosa, Eur. J. Inorg. Chem. **2016**, 832–843; b) J. J. Henkelis, C. J. Carruthers, S. E. Chambers, R. Clowes, A. I. Cooper, J. Fisher, M. J. Hardie, J. Am. Chem. Soc. **2014**, 136, 14393–14396; c) Z. Zhong, A. Ikeda, S. Shinkai, S. Sakamoto, K. Yamaguchi, Org. Lett. **2001**, 3, 1085–1087.

[9] CCDC 1486233 contain the supplementary crystallographic data for this paper. These data are provided free of charge by The Cambridge Crystallographic Data Centre.

[10] a) C.-T. Wang, L.-C. Shiu, K.-B. Shiu Chem.-Eur.J. **2015**, 21, 7026-7029; b) V. Chandrasekhar, T. Hajra, J. K. Bera, S. M. W. Rahaman, N. Satumtira, O. Elbjeirami, M. A. Omary, Inorg. Chem. **2012**, 51, 1319-1329; c) E. Baranoff, I. Jung, R. Scopelliti, E. Solari, M. Gratzel, Md. K. Nazeeruddin, Dalton Trans. **2011**, 40, 6860-6867; d) W.-S. Sie, G.-H. Lee, K. Y.-D. Tsai, I-J. Chang, K.-B. Shiu, J. Mol. Struct. **2008**, 890, 198-202.

[11] While NMR spectra of (±)-L1 remain unchanged with time, small additional peaks appear in the ^{1}H NMR spectra of CD_3NO_2-solutions of resolved L1 at room temperature (Fig. S2). This may be due to an unknown minor decomposition or saddle-like conformation from crown-saddle-crown racemisation, see for example G. Huber, T. Brotin, L. Dubois, H. Desvaux, J.-P. Dutasta, P. Berthault, J. Am. Chem. Soc. **2006**, 128, 6239-6246.

[12] J. J. Henkelis, J. Fisher, S. L. Warriner, M. J. Hardie, Chem. -Eur. J. **2014**, 20, 4117-4125.

[13] a) P. Bonakdarzadeh, F. Pan, E. Kalenius, O. Jurček, K. Rissanen, Angew. Chem. Int. Ed. **2015**, 54, 1480-14893; b) D. L. Caulder, R. E. Powers, T. N. Parac, K. N. Raymond, Angew. Chem. Int. Ed. **1998**, 37,

1840-1843. c) J. L. Bolliger, A. M. Belenguer, J. R. Nitschke, Angew. Chem. Int. Ed. **2013**, 52, 7958-7962; d) T. Liu, Y. Liu, W. Xuan, Y. Cui, Angew. Chem. Int. Ed. **2010**, 49, 4121-4124; e) S. P. Argent, T. Riis-Johannessen, J. C. Jeffery, L. P. Harding, M. D. Ward, Chem. Commun. **2005**, 4647-4649.

[14] a) S. A. Boer, D. R. Turner, Chem. Commun. **2015**, 51, 17375–17378; b) L.-L. Yan, C.-H. Tan, G.-L. Zhang, L.-P. Zhou, J.-C. Bünzli, Q.-F. Sun, J. Am. Chem. Soc. **2015**, 137, 8550–8555; c) C. Gütz, R. Hovorka, G. Schnakenburg, A. Lützen, Chem. Eur. J. **2013**, 19, 10890-10894; d) C. Maeda, T. Kamada, A. Osuka, Chem. Soc. Rev. **2007**, 251, 2743-2752.

[15] E. Baranoff, E. Orselli, L. Allouche, D. Di Censo, R. Scopelliti, M. Grätzel, M. K. Nazeeruddin, Chem. Commun. **2011**, 47, 2799-2801.